Pharmaceutical Sciences and Drug Design
ISSN: 3062-4428
2022, Volume 2, Page No: 212-224

Available online at: www.galaxypub.co/page/journals

Galaxy Publication

Galaxy Publication

Gui-Qi-Yi-Shen Granules Ameliorate IgA Nephropathy in Transgenic Mice by Suppressing TLR4/MyD88/NF-κB and IL-6/JAK2/STAT3 Signaling: An Integrated Network Pharmacology and Transcriptomic Study

Diana Brkovic[1]*, Marko Juric[1]

[1]Department of Phytochemistry, Faculty of Pharmacy, University of Zagreb, Zagreb, Croatia.

***E-mail** ✉ diana.brkovic.hr@gmail.com

Received: 09 September 2022; **Revised:** 01 December 2022; **Accepted:** 04 December 2022

ABSTRACT

IgA nephropathy (IgAN) remains a major cause of renal failure and mortality, and available treatments are still limited. Gui-qi-yi-shen (GQYS) granules—an established traditional Chinese medicinal formula—have long been used for IgAN, yet the molecular basis of their therapeutic effects is not fully defined. This study aimed to clarify how GQYS mediates its beneficial actions in IgAN. Eight-week-old Itgam-IRES-hCD89 mice were assigned to four experimental groups: IgAN, low-dose GQYS (GQYS-L, 5.2 g/kg), high-dose GQYS (GQYS-H, 10.4 g/kg), and Losartan (6.5 mg/kg). Age-matched C57/BL6 mice served as the control group. Therapeutic outcomes were assessed using periodic acid–Schiff (PAS) staining, serum and urine biochemical tests, and immunofluorescence (IF). To uncover mechanistic pathways, network pharmacology combined with transcriptomics was performed, followed by Western blotting and IF verification.

Relative to the IgAN model mice, both 24-hour proteinuria and alanine aminotransferase were significantly decreased in the GQYS-treated groups. PAS staining showed that mesangial cell proliferation and matrix accumulation—prominent features in IgAN—were less pronounced after GQYS intervention. IF analysis indicated reduced IgA and C3 deposition in the mesangial regions in comparison with untreated IgAN mice. Mechanistic prediction using network pharmacology and transcriptomics highlighted multiple genes and pathways potentially responsible for the actions of GQYS. Western blotting and IF confirmed that GQYS suppressed activation of the TLR4/MyD88/NF-κB and IL-6/JAK2/STAT3 signaling cascades. GQYS alleviates proteinuria and mitigates renal injury in IgAN, likely through modulation of TLR4/MyD88/NF-κB and IL-6/JAK2/STAT3 pathways, suggesting its promise as a therapeutic option.

Keywords: IgA nephropathy, Gui-qi-yi-shen granules, Kidney protection, TLR4 signaling, IL-6 pathway

How to Cite This Article: Brkovic D, Juric M. Gui-Qi-Yi-Shen Granules Ameliorate IgA Nephropathy in Transgenic Mice by Suppressing TLR4/MyD88/NF-κB and IL-6/JAK2/STAT3 Signaling: An Integrated Network Pharmacology and Transcriptomic Study. Pharm Sci Drug Des. 2022;2:212-24. https://doi.org/10.51847/auokZFw03z

Introduction

IgA nephropathy (IgAN) is the leading form of primary glomerulonephritis worldwide. Within 20–25 years of diagnosis, approximately 30–45% of affected individuals progress to end-stage renal disease (ESRD) [1]. Historically, IgAN therapy primarily relied on supportive measures. Although immunosuppressants can be beneficial, their use is restricted by adverse effects. In recent years, multiple targeted agents—such as SGLT-2 inhibitors, gut-directed budesonide (Nefecon), endothelin receptor antagonists, and complement-blocking therapies—have been approved for IgAN management [2, 3]. Despite these advances, limitations in efficacy, tolerability, and patient suitability persist, underscoring the urgent need for alternative strategies to slow IgAN progression and reduce ESRD incidence. Evidence from clinical practice suggests that traditional Chinese medicine can reduce proteinuria and improve inflammatory and fibrotic kidney injury in chronic kidney disease [4, 5].

Gui-qi-yi-shen (GQYS) granules originate from a classical prescription developed by Chinese medicine expert Yongjun Wang. The formulation contains five herbal components: Centella asiatica (L.) Urban (Jixuecao),

Astragalus membranaceus (Fisch.) Bunge (HuangQi), Rheum officinale Baill (DaHuang), Semen Persicae (TaoRen), and Angelica sinensis (Oliv.) Diels (DangGui). It is protected under China Patent Application 200510048997.9 and approved for hospital preparation (ZheYaoZhibeiZi: Z20240001000). The prescription is designed according to traditional principles—supporting qi and blood, promoting circulation, resolving stasis, eliminating symptoms, and dispelling wind and dampness—which correspond closely to the clinical characteristics and pathogenesis of IgAN. Clinical use of GQYS in IgAN has shown encouraging therapeutic benefits [6, 7], yet the precise biological mechanism remains insufficiently clarified and necessitates further foundational research.

In this investigation, we assessed the influence of GQYS on IgAN by employing Itgam-IRES-hCD89 transgenic mice, a model that reproduces the key renal abnormalities seen in patients—namely mesangial IgA accumulation, matrix enlargement, and modest proteinuria—comparable to the classical CD89 mouse line [8, 9]. By integrating network-based compound analysis, transcriptome profiling, and subsequent laboratory validation, our data indicate that GQYS chiefly protects renal tissue in IgAN through dampening the TLR4/MyD88/NF-κB cascade as well as the IL-6/JAK2/STAT3 axis. A schematic overview of the entire study workflow is presented in **Figure 1**, which outlines every stage of constituent profiling, pharmacological prediction, and functional experimentation.

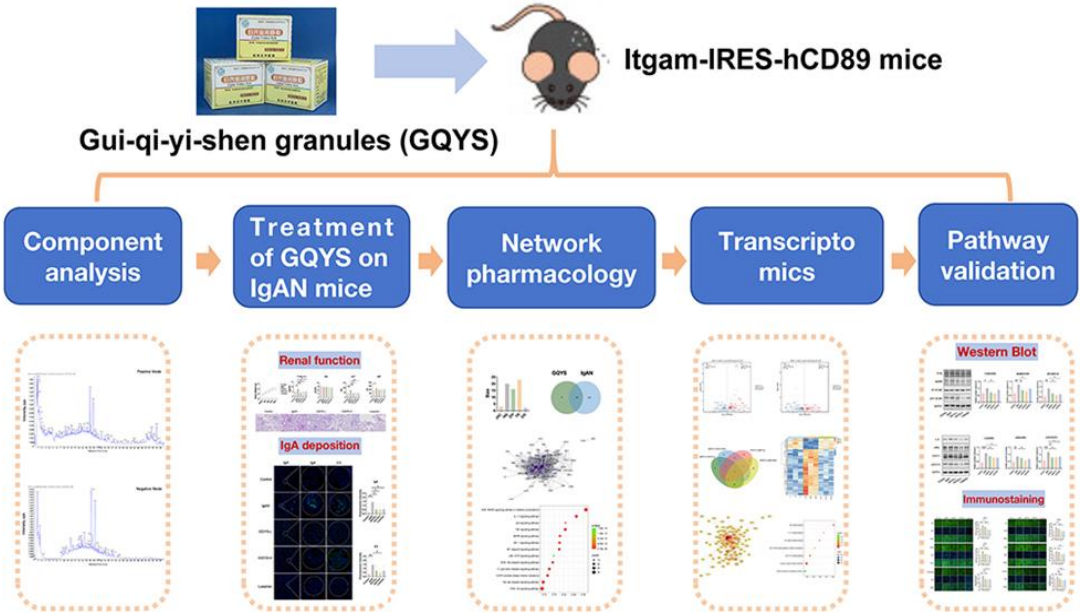

Figure 1. Diagram illustrating the overall research pipeline.

Materials and Methods

Reagents and drugs

GQYS preparations were supplied by the TCM Pharmacy of Hangzhou Hospital of Traditional Chinese Medicine. Losartan potassium (approval No. HJ20171081, Hangzhou) was sourced from Merck Sharp & Dohme Limited. Additional reagents included: PAS staining kit (G1281, Lot 2306001, Solarbio); Alexa Fluor® 488 goat anti-mouse IgA (1040-30, SouthernBiotech); FITC goat anti-mouse C3 (0855500, MP Biomedicals).

Primary antibodies comprised: TLR4 (19,811-1-AP), NF-κB p65 (10,745-1-AP), phospho-NF-κB p65 (10,745-1-AP), MyD88 (ab219413), IL-6 (A0286), JAK2 (ET1607-35), STAT3 (AF1492), phospho-STAT3 (ET-1607-39), and GAPDH (60004-1-Ig). Secondary antibodies (926-32,210 / 926-68071, LI-COR, USA), Alexa Fluor™ Plus 488 donkey anti-rabbit IgG (A32790), and DAPI (ab104139) were also used.

Component analysis

Chemical profiling of GQYS was carried out using UPLC-Q-TOF-MS/MS. A 1 g aliquot of granules was dissolved, adjusted to 20 mg/mL, filtered through a 0.22 μm membrane, and injected for analysis. Ionization was performed via ESI on a 7600 ZenoTOF High Definition mass spectrometer. Separation occurred on a Waters ACQUITY Cortecs T3 column (2.1 × 100 mm, 1.6 μm) with a matching guard column (2.1 × 50 mm, 1.6 μm). The mass spectrometer scanned 50–1500 Da. Sample injections were 5 μL, analyzed under a programmed

gradient. Column and autosampler temperatures were maintained at 50 °C and 4 °C, and the mobile phase (acetonitrile/0.1% formic acid–water) flowed at 0.35 mL/min.

Animals and treatments

A total of 40 male Itgam-IRES-hCD89 mice (eight weeks old; Cat. No. NM-KI-200063) were purchased from the Shanghai Model Organisms Center, while 10 age-matched male C57BL/6 mice served as the normal reference group. Animals were housed under SPF conditions. All procedures were approved by the Zhejiang Chinese Medical University Animal Research Committee (approval No. IACUC-20240311-07) and followed NIH guidelines.

After a 1-week acclimation period, the Itgam-IRES-hCD89 mice were assigned to four cohorts—IgAN, GQYS-L, GQYS-H, and Losartan—with 10 animals per group. The GQYS-L and GQYS-H mice received 5.2 g/kg and 10.4 g/kg GQYS by oral gavage. The 5.2 g/kg dosage corresponds to the adult clinical regimen (40 g/day), while the higher group received twice that amount. The Losartan group was treated with 6.5 mg/kg losartan potassium suspension. All doses were calculated using body-surface-area conversions from human therapeutic levels [10]. The intervention period lasted 5 months. Following completion, animals were sacrificed, and serum creatinine (Scr), 24 h protein excretion, and additional biochemical parameters were obtained using a Beckman Coulter Chemistry Analyzer. Kidneys were removed for subsequent experiments.

PAS staining

Kidney samples were fixed overnight in 10% formalin, embedded in paraffin, and cut into 2 μm sections for PAS staining. Images were later captured using a digital slide scanner (KF-PRO-020-HI; Konfoong Bioinformation Tech Co., Ltd., Zhejiang, China).

Network pharmacology analysis

Compounds contained in GQYS and their corresponding targets were obtained through the TCMSP platform (https://old.tcmsp-e.com/tcmsp.php). IgAN-related disease targets were collected from GeneCards, DisGeNET, and OMIM. A Venn diagram was generated with the jvenn tool (https://jvenn.toulouse.inrae.fr/app/example.html). The herb–compound–target interaction map was created in Cytoscape 3.7.2. The STRING database (http://string-db.org/) was used to construct the PPI network, which was subsequently displayed using Cytoscape.

Transcriptome analyses

Kidney tissue was pulverized in liquid nitrogen, and total RNA was isolated using TRIzol, following the provided protocol. RNA purity and concentration were checked using a NanoDrop 2000 (Thermo Scientific, USA), while RNA integrity was confirmed with an Agilent 2100 Bioanalyzer (Agilent Technologies, Santa Clara, CA, USA). Libraries were prepared using the VAHTS Universal V6 RNA-seq Library Prep Kit. Sequencing was carried out by OE Biotech, Inc. (Shanghai, China). Raw fastq files underwent QC using FastQC v0.11.9. Clean reads were aligned to the reference genome through HISAT2 (2.1.0). Gene FPKM values and read counts were generated by HTSeq-count (0.11.2). Differential gene analysis was conducted with DESeq2 (1.22.2), applying $Q < 0.05$ and log2 fold change > 1.2 as significance criteria. Further analyses used the OECloud platform (https://cloud.oebiotech.com). The transcriptome dataset is deposited in GEO (GSE286126).

Immunofluorescence analysis

Cryosections of kidneys (3 μm) were incubated with Alexa Fluor® 488- or FITC-labeled goat antibodies against mouse IgA and C3. Confocal images were obtained using a STELLARIS 5 microscope (Leica, Germany), and evaluations were made in a blinded manner with a DM2000 LED fluorescence microscope (Leica, Germany) ($n \geq 6$).

For signaling-related proteins, paraffin sections (3 μm) were treated with antibodies for TLR4, MyD88, pNF-κB, IL-6, JAK2, and pSTAT3, followed by an Alexa Fluor™ Plus 488 secondary antibody. After DAPI staining, slides were examined using an Operetta CLS high-content system (PerkinElmer, UK) and processed using ImageJ ($n = 6$).

Western blotting

Protein lysates from kidneys were prepared in chilled RIPA buffer, resolved via 10% or 15% SDS-PAGE, and blotted onto nitrocellulose membranes. Following incubation with primary and secondary antibodies, signal detection was performed with an Odyssey Scanner (LI-COR Biosciences, Lincoln, NE, USA). Band intensity quantification was carried out using ImageJ 1.52p (n = 6).

Statistical analysis

Statistical evaluations were conducted in GraphPad Prism 8.0.1. Data are shown as mean ± standard deviation. Comparisons among groups were analyzed using one-way ANOVA, with $p < 0.05$ considered statistically meaningful.

Results and Discussion

Component analysis of GQYS

To characterize the chemical profile of GQYS, UPLC-Q-TOF-MS/MS was applied. The total ion chromatograms in positive and negative ionization modes are displayed in **Figure 2**.

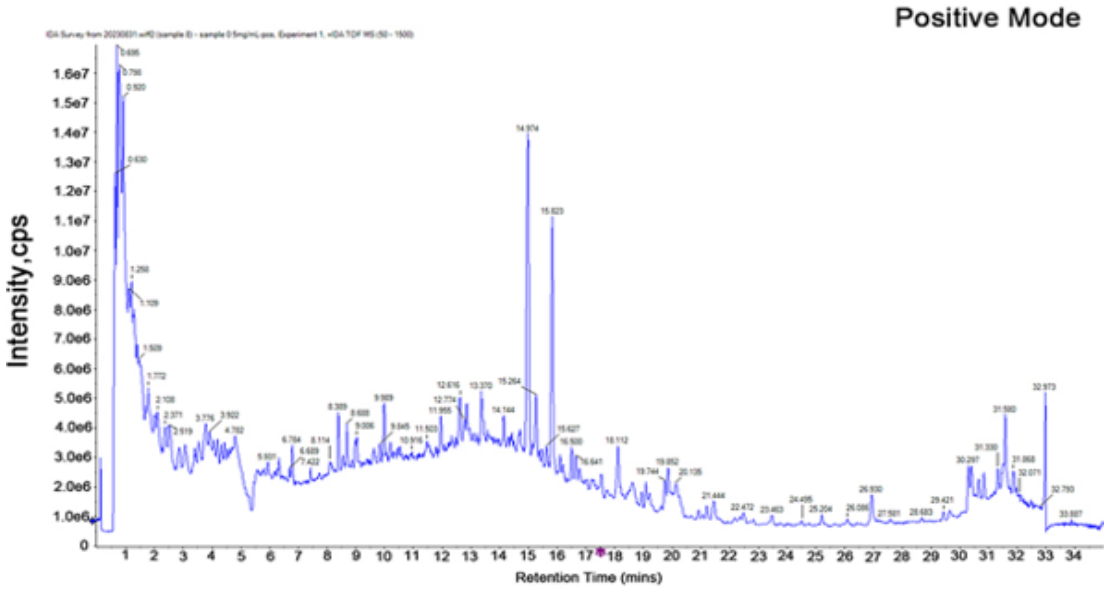

a)

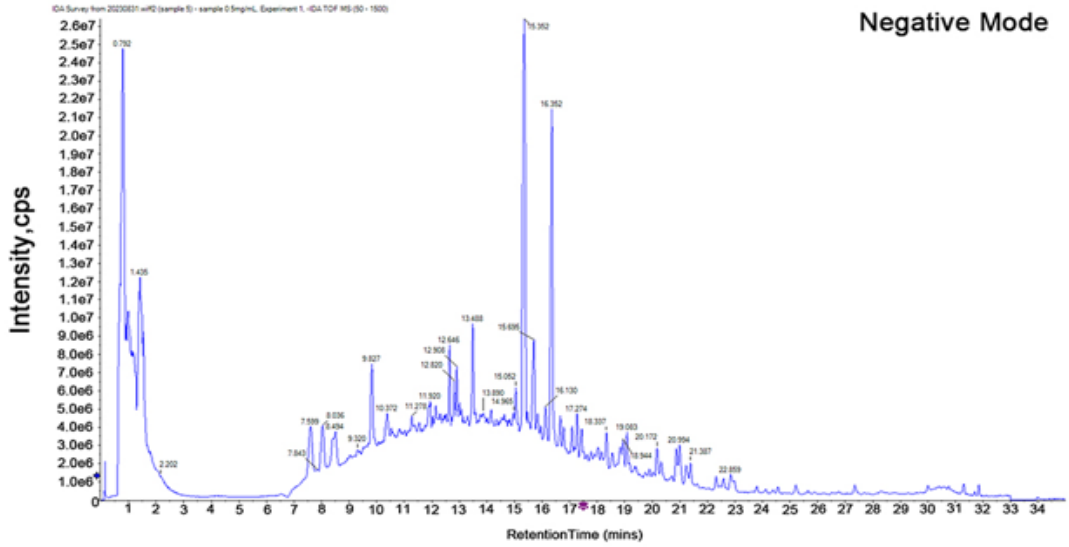

b)

Figure 2. Total ion chromatograms (TIC) of GQYS in positive (a) and negative (b) ion modes.

GQYS mitigated kidney damage in IgAN mice

Throughout the study period, the body weights of animals in each group remained relatively stable **(Figure 3a)**, suggesting that GQYS exhibited acceptable safety. Mice with IgAN showed marked increases in 24 h proteinuria, ALT, and AST when compared with healthy controls **(Figures 3b, 3d and 3e)**. Notably, the GQYS-L, GQYS-H, and Losartan groups showed significant reductions in 24 h proteinuria and ALT compared with the model group **(Figures 3b and 3d)**. SCr levels did not demonstrate major differences among groups **(Figure 3c)**. PAS staining indicated distinct mesangial cell proliferation and matrix expansion in IgAN mice, whereas these histopathologic alterations were evidently improved after treatment with GQYS-L, GQYS-H, or Losartan **(Figure 3f)**. Overall, the findings reveal a protective role of GQYS in renal injury.

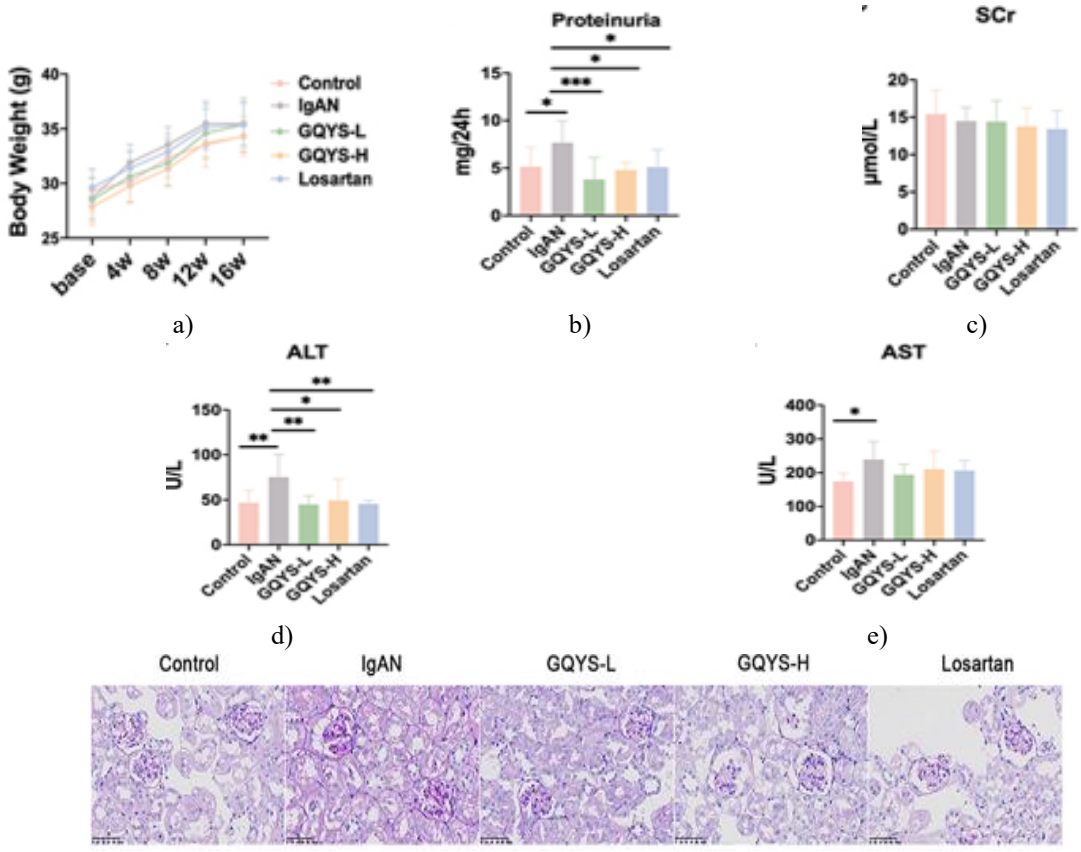

Figure 3. GQYS attenuates IgAN-induced renal damage. (a) Body weight changes during the experiment (n=10 per group). (b) Twenty-four-hour proteinuria (n=10). (c) SCr levels (n=10). (d) ALT (n=10). (e) AST (n=10). Results are expressed as mean ± SD. Statistical comparisons versus the IgAN group: *p < 0.05, **p < 0.01, ***p < 0.001. (f) Representative PAS-stained images (×400). Scale bar = 100 μm.

GQYS reduced mesangial IgA deposition in IgAN mice

As illustrated in **Figure 4**, IgAN mice displayed pronounced granular IgA accumulation within mesangial regions **(Figure 4a)**. In contrast, GQYS-L, GQYS-H, and Losartan treatment led to substantial decreases in IgA deposits **(Figures 4a and 4b)**. A similar trend was observed for C3, which was also prominently deposited in the model mice but decreased significantly after intervention. These observations imply that GQYS attenuates mesangial IgA deposition.

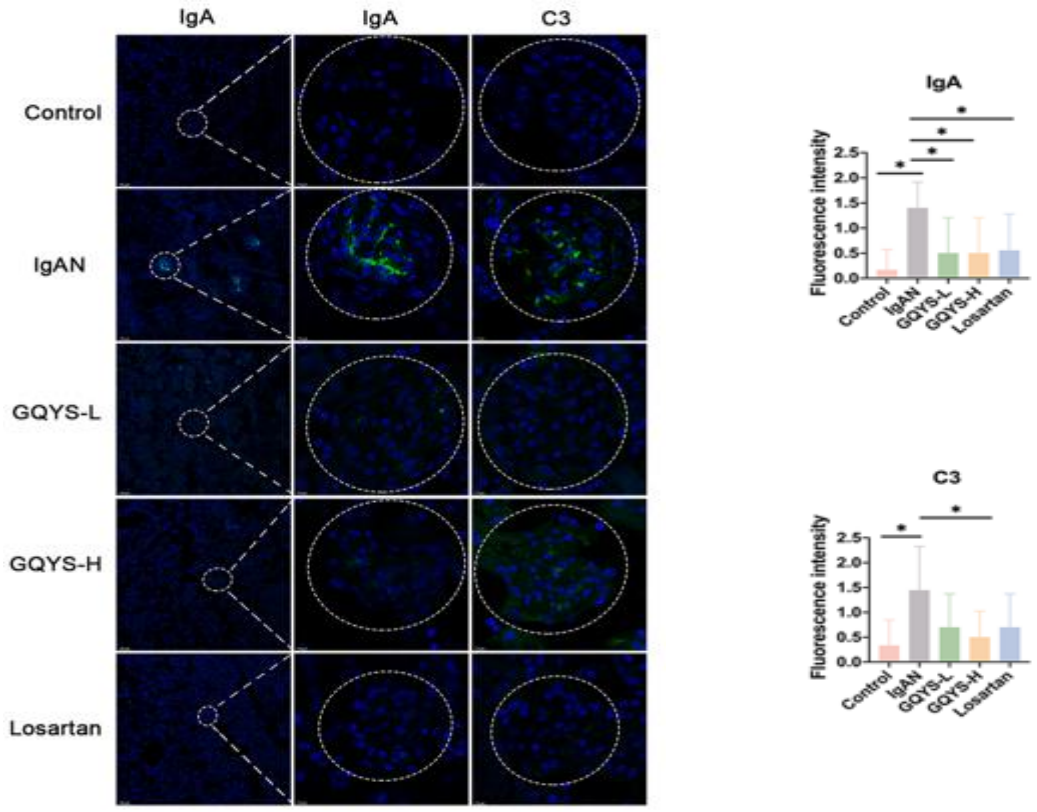

a) b)

Figure 4. GQYS reduces IgA deposition in the glomeruli of IgAN mice. (a) Immunofluorescence images for IgA and C3 with DAPI counterstaining. Scale bars: 50 μm (left), 7.5 μm (middle/right). (b) Blinded scoring of fluorescence intensity ($n \geq 6$). Values are shown as mean ± SD. Significance relative to IgAN: *$p < 0.05$.

Network pharmacology of GQYS active components and their targets

Using TCMSP data, 64 bioactive constituents were retrieved from five herbal components: Jixuecao, HuangQi, DaHuang, DangGui, and TaoRen. These herbs contributed 3, 20, 16, 23, and 2 compounds, respectively **(Figure 5a)**. Fifteen compounds lacked matched targets in TCMSP. Following removal of duplicates, 45 distinct compounds remained. In total, 214 non-redundant targets were captured, and the herb–compound–target network comprised 268 nodes and 889 edges. Among the compounds, quercetin (degree 158), kaempferol (58), 7-O-methylisomucronulatol (42), and formononetin (35) ranked highest, implying their potential importance in GQYS's therapeutic activity.

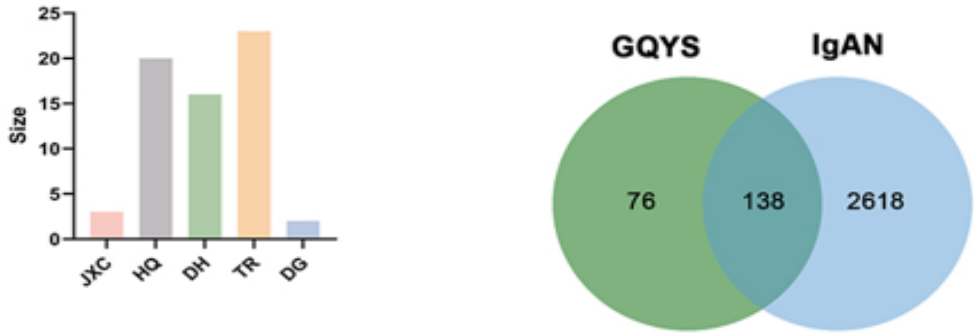

a) b)

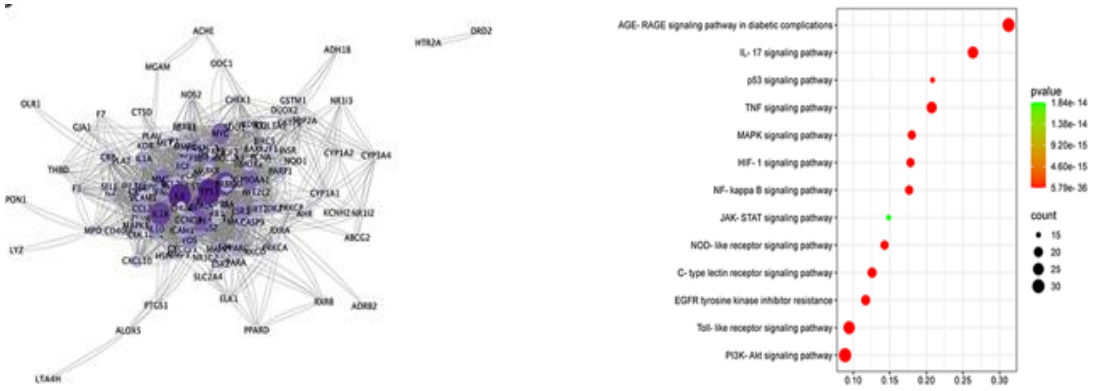

c) d)

Figure 5. Network pharmacology evaluation. (a) Distribution of active compounds among herbs. (b) Venn diagram for shared GQYS–IgAN targets. (c) Common-target PPI network. (d) Bubble diagram of major KEGG pathways.

IgAN-related genes were aggregated from GeneCards, OMIM, and DisGeNET, yielding 2756 unique disease targets. Intersecting these with GQYS targets identified 138 overlapping genes **(Figure 5b)**. A PPI network comprising 133 nodes and 2428 edges was generated **(Figure 5c)**. KEGG enrichment indicated involvement of signaling pathways such as PI3K-AKT, AGE-RAGE, TLR, TNF, and NF-κB **(Figure 5d)**.

Transcriptomic analysis of genes and pathways influenced by GQYS in IgAN

Between the control and IgAN groups, 267 DEGs were identified, including 196 upregulated and 71 downregulated transcripts **(Figure 6a)**. Comparing GQYS with IgAN mice, 503 DEGs were observed, of which 171 were upregulated and 332 were downregulated **(Figure 6b)**. A shared set of 155 genes displayed opposite expression patterns across the three groups **(Figure 6c)** and was visualized via a heatmap **(Figure 6d)**. The resulting PPI network included 94 nodes and 2428 interactions **(Figure 6e)**. KEGG pathway evaluation showed enrichment in cytokine-cytokine receptor interaction, JAK-STAT, TNF, and NF-κB pathways **(Figure 6f)**.

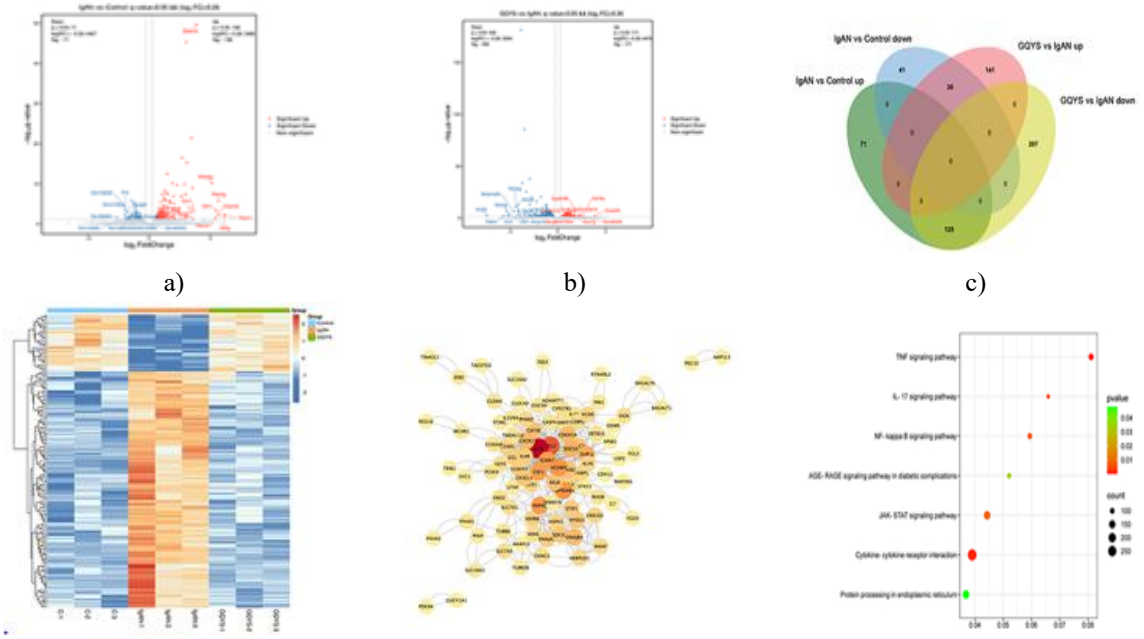

a) b) c)

d) e) f)

Figure 6. Transcriptomic profiling revealed gene sets and signaling routes linked to how GQYS acts in IgAN. (a) Volcano diagram showing gene-expression differences between the control and IgAN groups. (b) Volcano diagram illustrating DEGs comparing IgAN with GQYS treatment. (c) Venn chart presenting the shared and unique DEGs among control, IgAN, and GQYS groups. (d) Heatmap clustering DEGs across all

three groups. (e) Interaction network illustrating 155 overlapping DEGs. (f) KEGG enrichment of the same 155 genes.

GQYS influenced TLR4/MyD88/NF-κB and IL-6/JAK2/STAT3 pathways in IgAN mice

Findings from both network pharmacology and transcriptome assessments pointed to involvement of the TLR4/MyD88/NF-κB and IL-6/JAK2/STAT3 pathways, prompting experimental verification.

Immunofluorescence demonstrated that the TLR4 signal was primarily focused in the glomeruli, whereas MyD88, phosphorylated NF-κB, IL-6, JAK2, and phosphorylated STAT3 were detectable in glomerular and tubular compartments **(Figures 7 and 8)**. Relative to the IgAN group, mice receiving GQYS showed clear reductions in all of these markers. Western blot analysis supported these results: IgAN animals had sharply elevated protein levels of TLR4, MyD88, pNF-κB, IL-6, JAK2, and pSTAT3, and GQYS treatment substantially lowered their expression **(Figures 9 and 10)**. These observations suggest that GQYS modulates both major inflammatory signaling axes in IgAN.

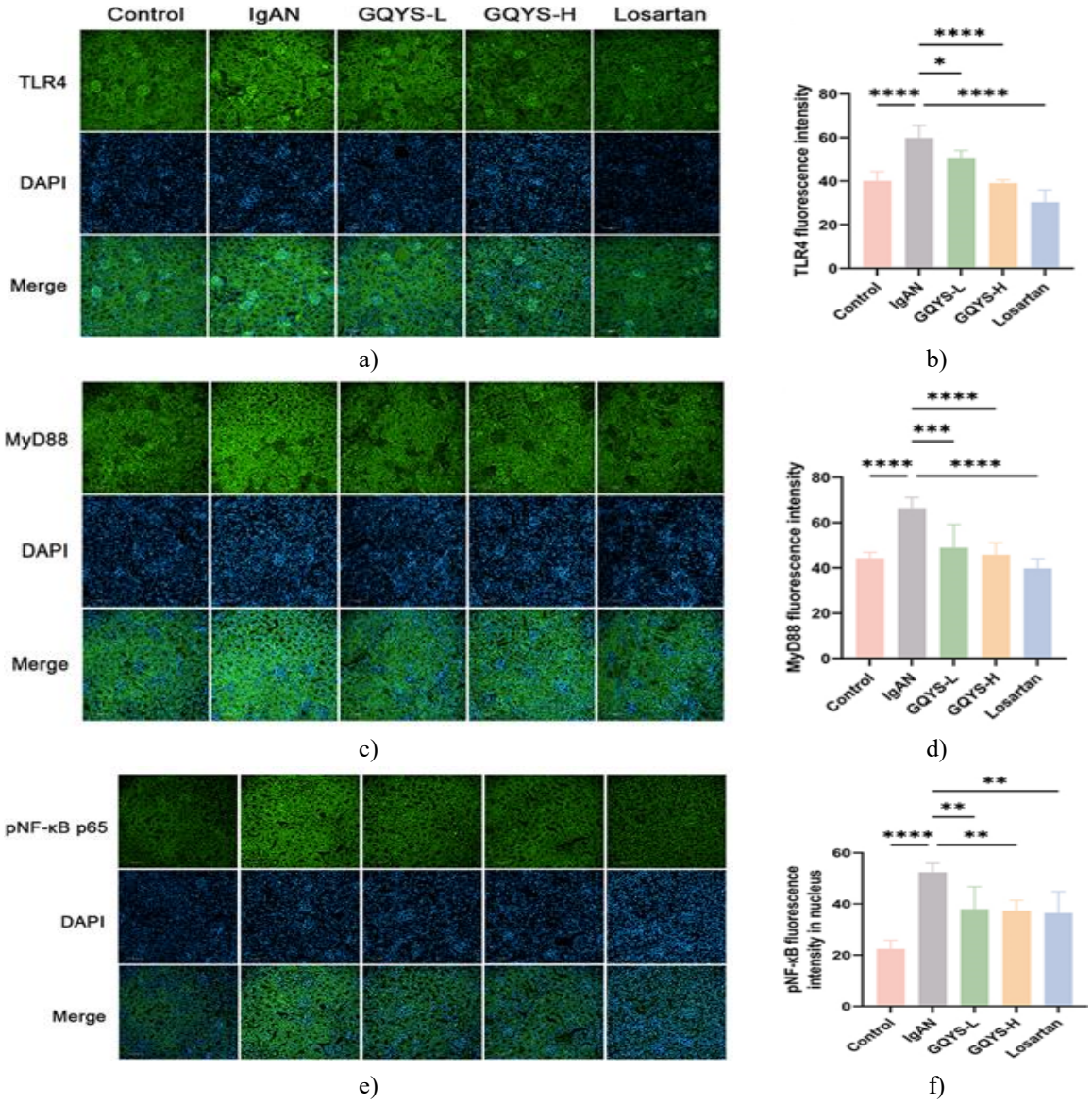

Figure 7. Immunofluorescent evaluation of the TLR4/MyD88/NF-κB axis. Panels show staining for TLR4 (a), MyD88 (c), and pNF-κB (e), with DAPI nuclear counterstaining. Scale bars = 100 μm. Quantitative fluorescence measurements of TLR4 (b), MyD88 (d), and pNF-κB (f) were obtained using ImageJ (n = 6). Results expressed as mean ± SD. Significance relative to IgAN: *p < 0.05, **p < 0.01, ***p < 0.001, ****p < 0.0001.

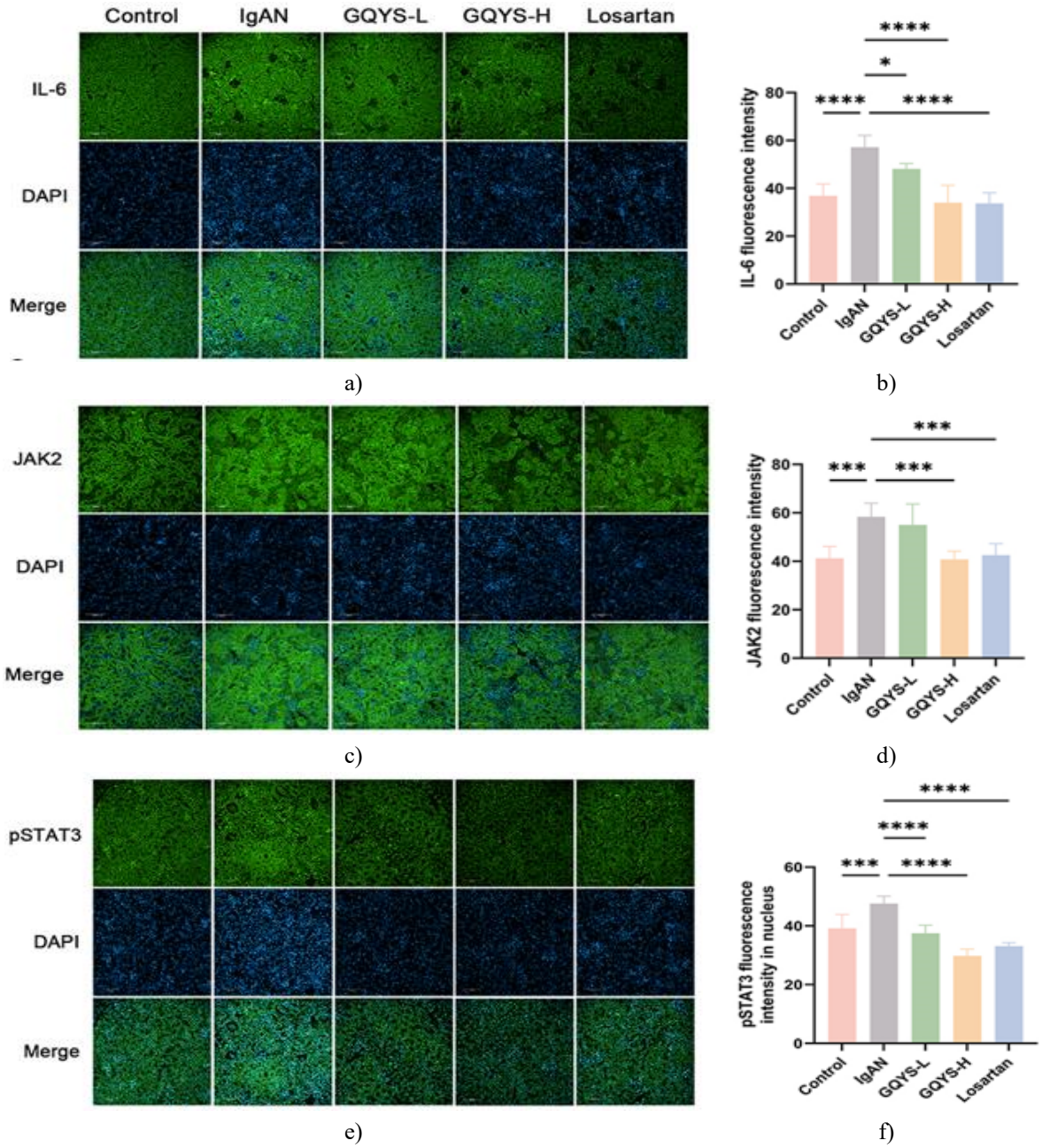

Figure 8. Immunofluorescent assessment of IL-6/JAK2/STAT3 activation. Staining patterns for IL-6 (a), JAK2 (c), and pSTAT3 (e), with DAPI-stained nuclei. Scale bars = 100 μm. Fluorescence intensities for IL-6 (b), JAK2 (d), and pSTAT3 (f) were quantified by ImageJ (n = 6). Data shown as mean ± SD. Statistical difference vs. IgAN: *p < 0.05, ***p < 0.001, ****p < 0.0001.

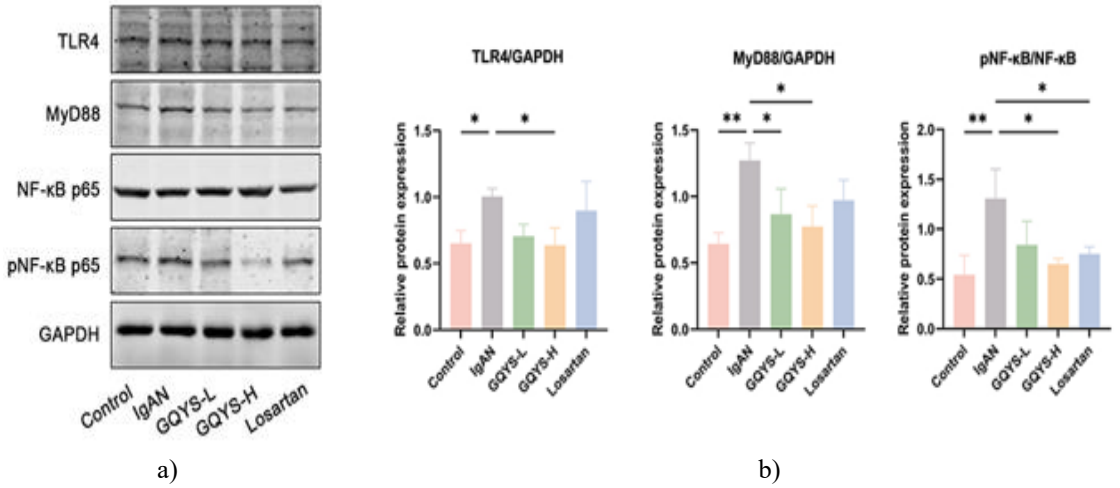

a) b)

Figure 9. Western blot examination of TLR4/MyD88/NF-κB signaling. (a) Protein bands for TLR4, MyD88, and pNF-κB. (b) Relative expression calculated by grayscale normalization to GAPDH (n = 6). Values shown as mean ± SD. Significance vs. IgAN: *p < 0.05, **p < 0.01.

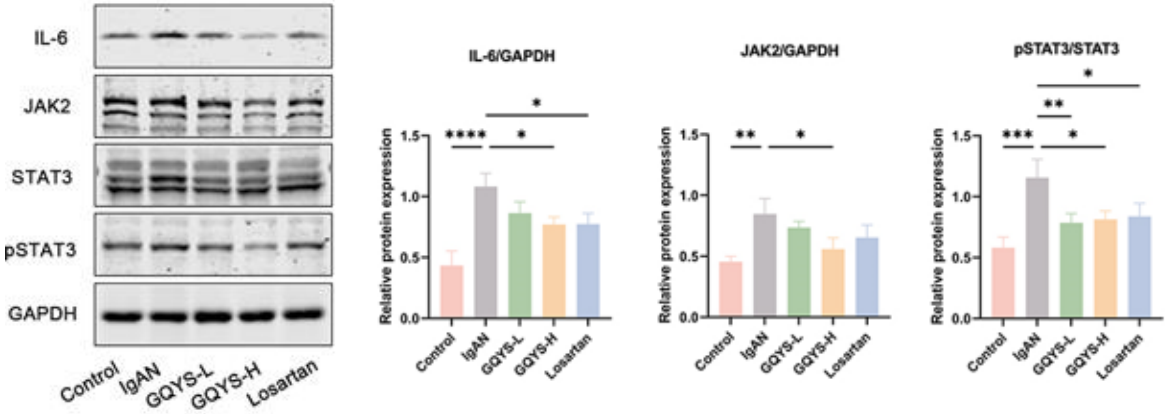

a) b)

Figure 10. Western blot evaluation of IL-6/JAK2/STAT3 signaling. (a) Protein bands for IL-6, JAK2, and pSTAT3. (b) Grayscale-derived relative levels normalized to GAPDH (n = 6). Mean ± SD displayed. Statistical comparison vs. IgAN: *p < 0.05, **p < 0.01, ***p < 0.001, ****p < 0.0001.

In this work, we employed Itgam-IRES-hCD89 mice, closely resembling the CD89 Tg strains described by Monteiro *et al*. [8, 9], in which CD89 expression is controlled by the CD11b promoter. By 20 weeks, these mice spontaneously developed substantial mesangial IgA accumulation, expansion of the mesangial matrix, and mild proteinuria. Therefore, the Itgam-IRES-hCD89 model reproduced fundamental IgAN-like lesions, making it suitable for examining how GQYS influences mesangial IgA build-up and proteinuria.

Traditional Chinese medicine features multi-compound, multi-target pharmacology, creating a complex therapeutic landscape. To elucidate GQYS's mode of action in IgAN, we implemented two integrated analytical approaches: one centered on chemical constituents and the other on biological pathways. First, mass spectrometry was used to define the primary molecules in GQYS. Then, potential active agents were screened through network pharmacology and the TCMSP platform, applying the thresholds oral bioavailability ≥30% and drug-likeness ≥1.8, and subsequently cross-referenced with the mass spectrometry profile. This process revealed three overlapping compounds—kaempferol, formononetin, and rhein—all exhibiting high network degrees, suggesting they may represent the major bioactive drivers of GQYS in IgAN. Each has been associated with modulation of inflammatory cascades. For instance, kaempferol is recognized for notable anti-inflammatory activity through NF-κB pathway regulation [11–13]. Rhein has been reported to improve IgAN and the condition of 5/6 nephrectomy rats by suppressing TLR4 signaling [14, 15]; additionally, it mitigates renal interstitial fibrosis via inhibition of STAT3 phosphorylation, thereby reducing tubular apoptosis [16]. Formononetin exerts protective

effects in rats experiencing inflammation from cerebral ischemia–reperfusion, mainly through the JAK2/STAT3 axis [17].

In addition, by merging network pharmacology with transcriptomic data, this study pinpointed multiple signaling pathways potentially involved in GQYS's therapeutic impact on IgAN, including PI3K-AKT, AGE-RAGE, Toll-like receptor, TNF, NF-κB, cytokine–cytokine receptor interactions, and JAK-STAT. On the basis of existing evidence regarding kaempferol, formononetin, and rhein, we concentrated specifically on validating the TLR4/MyD88/NF-κB and IL-6/JAK2/STAT3 pathways.

Toll-like receptors (TLRs) have been recognized as important contributors to innate immune activation and inflammatory processes [18, 19]. Among them, TLR4 signaling plays a particularly central role in driving mesangial injury and kidney fibrosis, largely by enhancing inflammatory mediator production in chronic renal disorders such as IgAN [20, 21]. Coppo *et al.* documented increased TLR4 levels in peripheral blood mononuclear cells from patients with IgAN [22], while He *et al.* demonstrated marked upregulation of TLR4 in rat IgAN models [23]. A key branch of TLR4 signaling involves the activation of NF-kB through a MyD88-dependent mechanism, which then elevates IL-6 and MCP-1 expression. This suggests that the TLR4 cascade represents a potential therapeutic target for alleviating IgAN. In Itgam-IRES-hCD89 mice, the TLR4/MyD88/NF-kB axis was significantly heightened, and GQYS therapy reversed this trend, implying that GQYS may mitigate IgAN by modulating inflammation mediated through this pathway.

A growing body of research has shown that IL-6 is a critical driver of IgAN pathophysiology [24, 25]. Earlier investigations revealed that IL-6 enhances Gd-IgA1 production in both IgA1-secreting human cells and murine IgAN models [26–28]. Elevated renal IL-6 levels in IgAN correlate with the extent of IgA accumulation and tissue injury [29, 30]. Furthermore, increased urinary IL-6 has been strongly linked with disease progression [31, 32]. Of the signaling routes activated downstream of IL-6, the JAK/STAT pathway is most prominent. In our IgAN model, proteins associated with the IL-6/JAK2/STAT3 cascade were markedly upregulated, whereas GQYS administration reduced their expression. These observations suggest that GQYS may help suppress inflammation and improve renal impairment in IgAN mice by blocking IL-6–related signaling.

This study has several limitations. First, inhibitors targeting the involved pathways were not utilized to further validate the mechanistic findings. Second, we did not include in vitro experiments using renal cell lines. Third, randomized clinical trial evidence for GQYS is not yet available, though our group is currently conducting such work. Notably, we have completed a retrospective analysis of 79 IgAN patients, which showed that GQYS significantly decreased serum creatinine and increased glomerular filtration rate (unpublished). We aim to provide more clinical data to substantiate GQYS's therapeutic potential.

Conclusion

This study investigates the therapeutic actions of GQYS on IgAN by integrating network pharmacology with transcriptomic analysis. Our findings indicate that GQYS may exert renal protective effects by inhibiting the TLR4/MyD88/NF-kB and IL-6/JAK2/STAT3 pathways. We anticipate that these results may offer a scientific foundation for developing new traditional Chinese medicine–based treatments and support future translational applications for IgAN therapy.

Acknowledgments: None

Conflict of Interest: None

Financial Support: None

Ethics Statement: None

References

1. Selvaskandan H, Barratt J, Cheung CK. Novel treatment paradigms: primary IgA nephropathy. Kidney Int Rep. 2024;9(2):203–13. doi:10.1016/j.ekir.2023.11.026
2. Floege J, Bernier-Jean A, Barratt J, Rovin B. Treatment of patients with IgA nephropathy: a call for a new paradigm. Kidney Int. 2025;107(4):640–51. doi:10.1016/j.kint.2025.01.014

3. Cheung CK, Alexander S, Reich HN, Selvaskandan H, Zhang H, Barratt J. The pathogenesis of IgA nephropathy and implications for treatment. Nat Rev Nephrol. 2025;21(1):9–23. doi:10.1038/s41581-024-00885-3
4. Ma S, Zhao M, Chang M, Shi X, Zhang Y, Shi Y. Effects and mechanisms of Chinese herbal medicine on IgA nephropathy. Phytomedicine. 2023;117:154913. doi:10.1016/j.phymed.2023.154913
5. Wang XH, Lang R, Liang Y, Zeng Q, Chen N, Yu RH. Traditional Chinese Medicine in treating IgA nephropathy: from basic science to clinical research. J Transl Int Med. 2021;9(3):161–7. doi:10.2478/jtim-2021-0021
6. Bao Z, Zhu C, Sun Y, Liao J, Chen H. Effects of Centella Asiatica Compound on renal expression of TNF-α and MIF in rats with IgA nephropathy. China J Tradition Chinese Med Pharm. 2019;34(08):3731–5.
7. Chen Y, Min J, Wu M, Yang R, Yu D. Therapeutic effect of the compound centella asiatica in patients with stages 4-5 CKD and its influence on serum α-Klotho and FGF23 levels. Clin Trad Med Pharmacol. 2025;6(1):200202. doi:10.1016/j.ctmp.2025.200202
8. Launay P, Grossetête B, Arcos-Fajardo M, Gaudin E, Torres SP, Beaudoin L, et al. Fcalpha receptor (CD89) mediates the development of immunoglobulin A (IgA) nephropathy (Berger's disease). Evidence for pathogenic soluble receptor-Iga complexes in patients and CD89 transgenic mice. J Exp Med. 2000;191(11):1999–2009. doi:10.1084/jem.191.11.1999
9. Wehbi B, Pascal V, Zawil L, Cogne M, Aldigier JC. History of IgA nephropathy mouse models. J Clin Med. 2021;10(14). doi:10.3390/jcm10143142
10. Nair AB, Jacob S. A simple practice guide for dose conversion between animals and human. J Basic Clin Pharm. 2016;7(2):27–31. doi:10.4103/0976-0105.177703
11. Kadioglu O, Nass J, Saeed ME, Schuler B, Efferth T. Kaempferol is an anti-inflammatory compound with activity towards NF-kappaB pathway proteins. Anticancer Res. 2015;35(5):2645–50.
12. Hosseini A, Alipour A, Baradaran Rahimi V, Askari VR. A comprehensive and mechanistic review on protective effects of kaempferol against natural and chemical toxins: role of NF-kappaB inhibition and Nrf2 activation. Biofactors. 2023;49(2):322–50. doi:10.1002/biof.1923
13. Park MJ, Lee EK, Heo HS, Kim MS, Sung B, Kim MK, et al. The anti-inflammatory effect of kaempferol in aged kidney tissues: the involvement of nuclear factor-kappaB via nuclear factor-inducing kinase/IkappaB kinase and mitogen-activated protein kinase pathways. J Med Food. 2009;12(2):351–8. doi:10.1089/jmf.2008.0006
14. Liu M, Wang L, Wu X, Gao K, Wang F, Cui J, et al. Rhein protects 5/6 nephrectomized rat against renal injury by reducing inflammation via NF-kappaB signaling. Int Urol Nephrol. 2021;53(7):1473–82. doi:10.1007/s11255-020-02739-w
15. Chen X, Peng S, Zeng H, Fu A, Zhu Q. Toll-like receptor 4 is involved in a protective effect of rhein on immunoglobulin A nephropathy. Indian J Pharmacol. 2015;47(1):27–33. doi:10.4103/0253-7613.150319
16. Chen Y, Mu L, Xing L, Li S, Fu S. Rhein alleviates renal interstitial fibrosis by inhibiting tubular cell apoptosis in rats. Biol Res. 2019;52(1):50. doi:10.1186/s40659-019-0257-0
17. Yu L, Zhang Y, Chen Q, He Y, Zhou H, Wan H, et al. Formononetin protects against inflammation associated with cerebral ischemia-reperfusion injury in rats by targeting the JAK2/STAT3 signaling pathway. Biomed Pharmacother. 2022;149:112836. doi:10.1016/j.biopha.2022.112836
18. Coppo R, Amore A, Peruzzi L, Vergano L, Camilla R. Innate immunity and IgA nephropathy. J Nephrol. 2010;23(6):626–32.
19. Lee M, Suzuki H, Ogiwara K, Aoki R, Kato R, Nakayama M, et al. The nucleotide-sensing toll-like receptor 9/toll-like receptor 7 system is a potential therapeutic target for IgA nephropathy. Kidney Int. 2023;104(5):943–55. doi:10.1016/j.kint.2023.08.013
20. Zou JN, Xiao J, Hu SS, Fu CS, Zhang XL, Zhang ZX, et al. Toll-like receptor 4 signaling pathway in the protective effect of pioglitazone on experimental immunoglobulin A nephropathy. Chin Med J. 2017;130(8):906–13. doi:10.4103/0366-6999.204101
21. Liusheng LI, Mingming ZH, Yuan SI, Jinning ZH, Bin YA. Protective effect of modified Huangqi Chifeng decoction on immunoglobulin A nephropathy through toll-like receptor 4/myeloid differentiation factor 88/nuclear factor-kappa B signaling pathway. J Tradit Chin Med. 2024;44(2):324–33. doi:10.19852/j.cnki.jtcm.20240203.001

22. Coppo R, Camilla R, Amore A, Peruzzi L, Daprà V, Loiacono E, et al. Toll-like receptor 4 expression is increased in circulating mononuclear cells of patients with immunoglobulin A nephropathy. Clin Exp Immunol. 2010;159(1):73–81. doi:10.1111/j.1365-2249.2009.04045.x
23. He L, Peng X, Liu G, Tang C, Liu H, Liu F, et al. Anti-inflammatory effects of triptolide on IgA nephropathy in rats. Immunopharmacol Immunotoxicol. 2015;37(5):421–7. doi:10.3109/08923973.2015.1080265
24. Groza Y, Jemelkova J, Kafkova LR, Maly P, Raska M. IL-6 and its role in IgA nephropathy development. Cytokine Growth Factor Rev. 2022;66:1–14. doi:10.1016/j.cytogfr.2022.04.001
25. Taniguchi Y, Yorioka N, Kumagai J, Katsutani M, Kuratsune M, Amimoto D, et al. Interleukin-6 localization and the prognosis of IgA nephropathy. Nephron. 1999;81(1):94–8. doi:10.1159/000045254
26. Suzuki H, Raska M, Yamada K, Moldoveanu Z, Julian BA, Wyatt RJ, et al. Cytokines alter IgA1 O-glycosylation by dysregulating C1GalT1 and ST6GalNAc-II enzymes. J Biol Chem. 2014;289(8):5330–9. doi:10.1074/jbc.M113.512277
27. Yamada K, Huang ZQ, Raska M, Reily C, Anderson JC, Suzuki H, et al. Inhibition of STAT3 signaling reduces IgA1 autoantigen production in IgA nephropathy. Kidney Int Rep. 2017;2(6):1194–207. doi:10.1016/j.ekir.2017.07.002
28. Makita Y, Suzuki H, Kano T, Takahata A, Julian BA, Novak J, et al. TLR9 activation induces aberrant IgA glycosylation via April- and IL-6-mediated pathways in IgA nephropathy. Kidney Int. 2020;97(2):340–9. doi:10.1016/j.kint.2019.08.022
29. Rops AL, Jansen E, van der Schaaf A, Pieterse E, Rother N, Hofstra J, et al. Interleukin-6 is essential for glomerular immunoglobulin A deposition and the development of renal pathology in Cd37-deficient mice. Kidney Int. 2018;93(6):1356–66. doi:10.1016/j.kint.2018.01.005
30. Lim CS, Yoon HJ, Kim YS, Ahn C, Han JS, Kim S, et al. Clinicopathological correlation of intrarenal cytokines and chemokines in IgA nephropathy. Nephrology. 2003;8(1):21–7. doi:10.1046/j.1440-1797.2003.00128.x
31. Zhao W, Feng S, Wang Y, Wang C, Ren P, Zhang J, et al. Elevated urinary IL-6 predicts the progression of IgA nephropathy. Kidney Int Rep. 2023;8(3):519–30. doi:10.1016/j.ekir.2022.12.023
32. Harada K, Akai Y, Kurumatani N, Iwano M, Saito Y. Prognostic value of urinary interleukin 6 in patients with IgA nephropathy: an 8-year follow-up study. Nephron. 2002;92(4):824–6. doi:10.1159/000065465